Cellular/Molecular

Phosphoinositides Regulate $P2X_4$ ATP-Gated Channels through Direct Interactions

Louis-Philippe Bernier,[1] Ariel R. Ase,[1] Stéphanie Chevallier,[1] Dominique Blais,[1] Qi Zhao,[2] Éric Boué-Grabot,[3] Diomedes Logothetis,[2] and Philippe Séguéla[1]

[1]Montreal Neurological Institute, Department of Neurology and Neurosurgery, McGill University, Montréal, Québec, Canada H3A 2B4, [2]Department of Structural and Chemical Biology, Mount Sinai School of Medicine, New York University, New York, New York 10029, and [3]Université de Bordeaux 2, Centre National de la Recherche Scientifique, Unité Mixte de Recherche 5227, 33076 Bordeaux, France

P2X receptors are ATP-gated nonselective cation channels highly permeable to calcium that contribute to nociception and inflammatory responses. The $P2X_4$ subtype, upregulated in activated microglia, is thought to play a critical role in the development of tactile allodynia following peripheral nerve injury. Posttranslational regulation of $P2X_4$ function is crucial to the cellular mechanisms of neuropathic pain, however it remains poorly understood. Here, we show that the phosphoinositides $PI(4,5)P_2$ (PIP_2) and $PI(3,4,5)P_3$ (PIP_3), products of phosphorylation by wortmannin-sensitive phosphatidylinositol 4-kinases and phosphatidylinositol 3-kinases, can modulate the function of native and recombinant $P2X_4$ receptor channels. In BV-2 microglial cells, depleting the intracellular levels of PIP_2 and PIP_3 with wortmannin significantly decreased $P2X_4$ current amplitude and $P2X_4$-mediated calcium entry measured in patch clamp recordings and ratiometric ion imaging, respectively. Wortmannin-induced depletion of phosphoinositides in *Xenopus* oocytes decreased the current amplitude of $P2X_4$ responses by converting ATP into a partial agonist. It also decreased their recovery from desensitization and affected their kinetics. Injection of phosphoinositides in wortmannin-treated oocytes reversed these effects and application of PIP_2 on excised inside-out macropatches rescued $P2X_4$ currents from rundown. Moreover, we report the direct interaction of phospholipids with the proximal C-terminal domain of $P2X_4$ subunit (Cys_{360}–Val_{375}) using an *in vitro* binding assay. These results demonstrate novel regulatory roles of the major signaling phosphoinositides PIP_2 and PIP_3 on $P2X_4$ function through direct channel–lipid interactions.

Key words: **P2X; purinergic; PIP_2; calcium; microglia; neuropathic pain**

Introduction

Mammalian P2X receptors are ATP-gated nonselective cation channels, generated from the trimeric assembly of homologous subunits ($P2X_{1–7}$). Each subunit is composed of two transmembrane domains connected by a large ectodomain, with both N and C termini facing the intracellular side of the plasma membrane (North, 2002). In the nervous system, P2X receptor channels are expressed at the plasma membrane of neurons, astrocytes, and microglia, where they contribute to intercellular purinergic communication.

The $P2X_4$ subunit forms a functional homomeric channel with high permeability to calcium ions (Egan and Khakh, 2004). It can also heteromerize with $P2X_1$ (Nicke et al., 2005), $P2X_6$ (Lê et al., 1998), or $P2X_7$ subunits (Guo et al., 2007). It is expressed at high levels in central neurons and in microglial cells (Lê et al., 1998; Rubio and Soto, 2001; Tsuda et al., 2003). In recent years, microglial $P2X_4$ receptor channels have been found to play a critical role in the development of neuropathic pain induced by peripheral nerve injury (Tsuda et al., 2003; Inoue et al., 2004; Trang et al., 2006). The upregulation of $P2X_4$ expression in activated microglia following nerve injury is critical to the development of tactile allodynia (Tsuda et al., 2003) via the release of microglial BDNF and KCC2 cotransporter-mediated disinhibition of dorsal horn neurons (Coull et al., 2003, 2005). Despite the involvement of the $P2X_4$ receptor subtype in the pathogenesis of chronic pain, very little is known about its posttranslational regulation.

A lot of attention has been brought to phosphoinositides as modulators of membrane proteins. These phospholipids are produced by the combinatorial action of selective lipid kinases, namely phosphoinositol 3-kinase (PI3K), phosphoinositol 4-kinase (PI4K) and phosphoinositol 5-kinase, which phosphorylate the inositol ring at the 3′, 4′, or 5′ positions. Synthesis of the major phosphoinositide $PI(4,5)P_2$ (PIP_2) is completed through successive phosphorylations by PI4K and phosphoinositol(4)5-kinase. Formation of $PI(3,4,5)P_3$ (PIP_3) from PIP_2 necessitates one additional phosphorylation by PI3K. Phosphoinositides are regulators of several important cellular processes, such as vesicle trafficking, cytoskeleton remodeling, and ion channel function (Hilgemann et al., 2001; Suh and Hille, 2005). Interestingly, it has been shown that $P2X_1$, $P2X_2$, and $P2X_7$ receptors are positively

Received July 1, 2008; revised Oct. 10, 2008; accepted Oct. 14, 2008.

This work has been supported by operating grants from Canadian Institutes of Health Research (CIHR) (P.S.), Agence Nationale pour la Recherche and Projet International de Coopération Scientifique du Centre National de la Recherche Scientifique (E.B.G.), and National Institutes of Health (D.L.). L.P.B. holds a studentship from the CIHR training grant "Pain: Molecules to Community."

Correspondence should be addressed to Dr. Philippe Séguéla, Montreal Neurological Institute, 3801 University, Suite 778, Montréal, Québec, Canada H3A 2B4. E-mail: philippe.seguela@mcgill.ca.

DOI:10.1523/JNEUROSCI.3038-08.2008

 0270-6474/08/2812938-08$15.00/0

modulated by different phosphoinositides (Fujiwara and Kubo, 2006; Zhao et al., 2007; Bernier et al., 2008).

Phosphoinositides can interact with membrane proteins via electrostatic binding to positively charged residues (Rosenhouse-Dantsker and Logothetis, 2007). The $P2X_4$ subunit contains a phosphoinositide-binding motif characterized by a cluster of lysine and arginine residues in the intracellular C-terminal domain in close proximity to its second transmembrane domain. In this study, we used electrophysiological techniques to elucidate the role major phosphoinositides play in the modulation of microglial and recombinant $P2X_4$ receptor channel function. We also investigated the impact of phosphoinositides on $P2X_4$-mediated calcium entry and the structural characteristics of their interactions with $P2X_4$ using a lipid binding assay.

Materials and Methods

Patch-clamp recordings in BV-2 cells. Mouse BV-2 microglial cells were a kind gift from Dr. Jean Labrecque (AstraZeneca R&D) and were routinely maintained at 37°C and 5% CO_2 in DMEM supplemented with 5% heat-inactivated FBS, 10 mM pyruvate (Sigma), 5% L-glutamine (Invitrogen), penicillin, and streptomycin. Whole-cell patch-clamp recordings of BV-2 cells ($V_{hold} = -60$ mV) were performed using pipettes filled with internal solution, pH 7.2, containing (in mM) 120 K-gluconate, 1 $MgCl_2$, 4 NaOH, and 10 HEPES. The normal recording solution, pH 7.4, comprised (in mM) 130 NaCl, 5 NaOH, 3 KCl, 1 $MgCl_2$, 2 $CaCl_2$, and 10 HEPES. Low divalent recording solution contained 0.3 mM $CaCl_2$ without Mg^{2+}. Membrane currents were recorded using an Axopatch 200B amplifier and digitized at 500 Hz with a Digidata 1330 interface (Axon Instruments). Drugs were dissolved in recording solution and applied using a SF-77B fast perfusion system (Warner Instruments) at a rate of 1 ml/min. All experiments were performed at room temperature.

Ratiometric measurement of $[Ca^{2+}]_i$ in BV-2 cells. BV-2 cells were loaded with Ca^{2+}-sensitive fluorescent dye fura-2 AM (5 μM, Molecular Probes) in Ringer's solution (in mM: 130 NaCl, 3 KCl, 2 $CaCl_2$, 1 $MgCl_2$, 10 HEPES; 37°C, pH 7.4) with 1% BSA for 30 min at 37°C in the dark. Cells were washed three times to remove extracellular fura-2 AM and left for at least 30 min for complete hydrolysation of acetoxymethyl ester before imaging. Fluorescence measurement of Ca^{2+} in individual cells were performed on an inverted TE2000-U microscope (Nikon) equipped with 40× oil-immersion objective [CFI super(S) fluor, Nikon]. Fura-2 AM was excited alternatively at 340 and 380 nm with a Lambda 10-2 filter wheel (Sutter Instrument) coupled to a xenon arc lamp (XPS-100, Nikon). The fluorescent emission was monitored at 510 nm and recorded by a high-resolution cooled CCD camera (Cool Snap-HQ, Roper Scientific/Photometrics) interfaced to a Pentium III PC. Pairs of 340 and 380 nm images were acquired every second and ratio images were calculated using Metafluor 7.0 software (Molecular Devices). The experiment was performed at room temperature. Cells were superfused with Ringer's solution and drugs at a flow rate of 1 ml/min. Results were expressed as the 340/380 nm emission ratio proportional to the intracellular calcium. The magnitude of responses to ATP was calculated as the difference between the peak of the response and the basal ratio (Δ ratio). To test the viability of the cells, they were challenged with 1 μM ionomycin at the end of each recording. In each experiment, all conditions were tested (control, ivermectin, and ivermectin plus wortmannin) and data were collected from 3 independent experiments.

Two-electrode voltage clamp recordings in Xenopus *oocytes.* Oocytes were surgically removed from Tricaine-anesthetized female *Xenopus laevis* frogs and were incubated in OR2 solution containing 1–2 mg/ml type IA collagenase at room temperature for 2 h under vigorous agitation. Stage V and VI oocytes were then manually defolliculated before intranuclear microinjection of plasmid DNA coding for $rP2X_4$ (3 ng). After injection, oocytes were incubated in Barth's solution containing 1.8 mM $CaCl_2$ at 19°C for 24 to 72 h before electrophysiological recordings. Two-electrode voltage-clamp recordings ($V_{hold} = -60$ mV) were performed using glass pipettes (1–3 MΩ) filled with 3 M KCl solution. Oocytes were placed in a recording chamber and perfused at a flow rate of 10 to 12 ml/min with Ringer's solution, pH 7.4, containing (in mM) 115 NaCl, 5 NaOH, 2.5 KCl, 1.8 $CaCl_2$, and 10 HEPES. Membrane currents (d.c., 1 kHz) were recorded using a Warner OC-725B amplifier (Warner Instrument) and digitized at 500 Hz. Agonists were dissolved in the perfusion solution and applied using a computer-driven valve system. All series of recordings consisted of three successive applications of ATP 100 μM, with a 4 min washout with Ringer's solution between each application.

Macropatch recordings in Xenopus *oocytes.* Inside-out macropatch experiments were performed using an Axopatch 200B amplifier (Axon Instruments). PClamp 9 was used for data acquisition and analysis. The vitelline membrane of *Xenopus* oocytes was removed using fine forceps before recordings. Electrodes with resistance of 0.5–1.0 MΩ were used. The currents were evoked by ramps from +100 mV to −100 mV. The time course of the currents at −80 mV was analyzed. The pipette solutions contained 100 μM ATP and dioctanoyl (diC_8)-PIP_2 (5 μM) was dissolved in the bath solution. The solutions were applied through a gravity-driven perfusion system. For each experiment, a minimum of two batches of oocytes were tested.

Lipid binding assay. Oligonucleotides coding for amino acid sequences proximal to the C terminus (C_{360}–V_{375}) or the N terminus (F_{12}–V_{29}) of $P2X_4$ were inserted into the pGEX-2T vector (New England Biolabs) for the production of the corresponding recombinant GST fusion proteins. The lipid binding analysis of the GST-fusion proteins was conducted using lipid coated hydrophobic membranes (PIP Strips, Echelon Biosciences). The membranes were first blocked with TBS+T solution supplemented with 3% BSA for 1 h at room temperature. The membranes were then incubated overnight in TBS+T with 3% BSA and 1 μg/ml GST fusion protein. The membranes were then washed with TBS+T six times, 5 min per wash. The primary antibody (mouse anti-GST, 1:1000) was then added in TBS+T, 3% BSA solution for 1 h. Washes with TBS+T were repeated, followed by incubation with the secondary antibody (goat anti-mouse HRP, 1:5000) in TBS+T, 3% BSA. The membranes were washed again in TBS+T, then bound proteins were detected in ECL.

Data analysis. Peak currents, defined as the maximal amplitude recorded during agonist application, were measured for comparative analysis. For recovery experiments, the amplitude of the third response was compared with the first and expressed as a percentage. The results obtained after a 2 h drug incubation were always compared with those obtained after a 2 h control incubation in Barth's solution containing vehicle (100 nM or 35 μM DMSO). For current kinetics experiments, activation rate was measured as the rise time (in seconds) from 10% to 90% of the peak amplitude. For desensitization rate, the time constant was measured with a one-exponential fit of the inactivation phase of the current. Data are presented as mean ± SEM and analyzed using Student's *t* test or one-way ANOVA followed by a Bonferroni's multiple comparison test. Normalized data were analyzed using nonparametric Mann–Whitney test.

Results

Depletion of phosphoinositides decreases $P2X_4$ current density in BV-2 microglial cells

To assess the role phosphoinositides might play on native $P2X_4$ currents, we tested the effect of blocking PIP_2 and/or PIP_3 synthesis with wortmannin in BV-2 microglial cells. The furanosteroid wortmannin has been extensively used to block key lipid kinases in the phosphoinositides synthesis pathways. It is a potent inhibitor of PI3K at nanomolar concentrations while it blocks also PI4K at micromolar concentrations (Nakanishi et al., 1995; Vanhaesebroeck et al., 2001). Murine BV-2 cells express endogenous $P2X_4$ and $P2X_7$ channels (Raouf et al., 2007). To isolate $P2X_4$ currents from $P2X_7$ currents, we took advantage of the differential agonist sensitivity of the mouse $P2X_4$ and $P2X_7$ subtypes. Mouse $P2X_7$ receptors exhibit a markedly lower sensitivity to the agonist ATP than the mouse $P2X_4$ subtype (ATP EC_{50} >500 μM and <10 μM respectively) (Townsend-Nicholson et al., 1999). Ivermectin is an allosteric modulator of $P2X_4$ receptors that enhances currents by stabilizing the agonist-induced open

state (Priel and Silberberg, 2004). Therefore, ivermectin provides an additional tool to isolate $P2X_4$ currents from microglial cells. Application of 100 μM ATP evoked ivermectin-potentiated inward currents typical of the $P2X_4$ subtype (Fig. 1*A*). Vehicle-treated cells showed an ATP-evoked current density of 1.7 ± 0.3 pA/pF, while current density following 3 μM ivermectin treatment was increased to 13.9 ± 2.2 pA/pF ($p < 0.0001$, $n = 9$–10) (Fig. 1*A*,*B*). Depletion of PIP_3 levels with 100 nM wortmannin (PI3K blockade) for 2 h led to a significant decrease of ivermectin-potentiated $P2X_4$ current density (6.3 ± 0.6 pA/pF; $p = 0.0096$, $n = 7$). A comparable decrease was observed by blocking both PI3K and PI4K with 35 μM wortmannin for 2 h when compared with ivermectin alone (4.2 ± 0.9 pA/pF; $p = 0.0025$, $n = 7$).

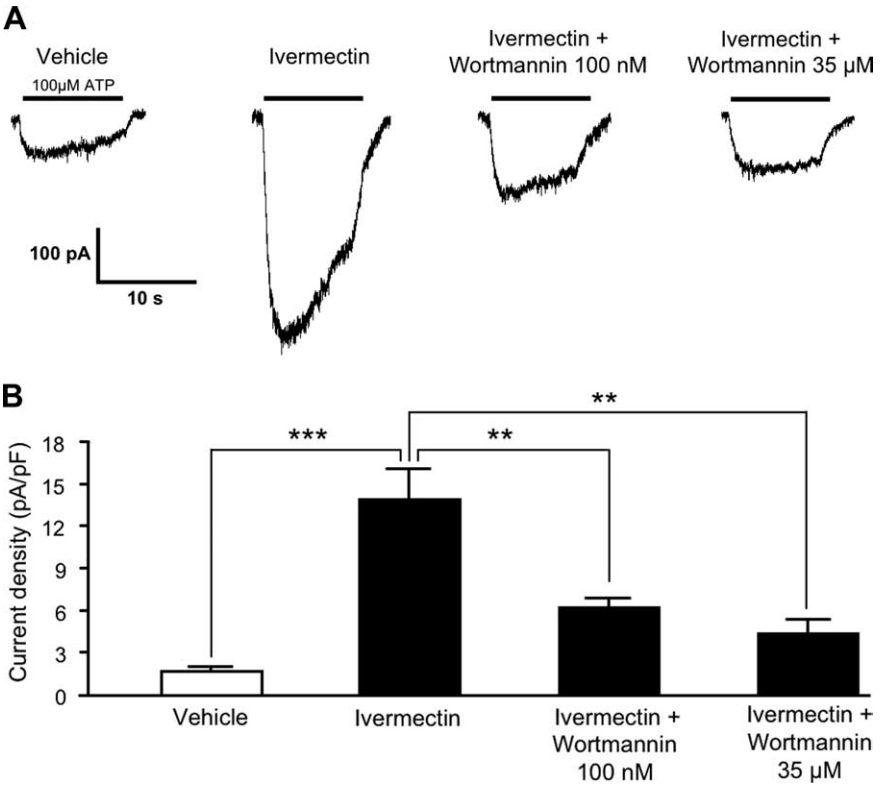

Figure 1. Blocking phosphoinositide synthesis with wortmannin leads to a decrease in $P2X_4$ current amplitude in microglial BV-2 cells. BV-2 cells were stimulated with 100 μM ATP to evoke inward $P2X_4$ currents. ***A***, Sample traces of $P2X_4$ currents after BV-2 cells were treated with vehicle (DMSO), 3 μM ivermectin, or 3 μM ivermectin with 100 nM or 35 μM wortmannin. ***B***, Ivermectin treatment led to an increase in current density, the means before and after ivermectin were 1.70 ± 0.27 and 13.90 ± 2.19 pA/pF, respectively ($p < 0.0001$, $n = 9$–10). Treatment with 100 nM or 35 μM wortmannin led to a decrease in current density to 6.25 ± 0.58 pA/pF ($p = 0.0096$, $n = 7$) and 4.21 ± 0.94 pA/pF ($p = 0.0025$ $n = 7$), respectively.

$P2X_4$-mediated calcium entry is sensitive to depletion of phosphoinositides

Taking advantage of the fact that $P2X_4$ receptor channels are highly calcium permeable (Egan and Khakh, 2004), we used ratiometric fura-2 fluorescence imaging to measure changes in intracellular calcium concentration ($[Ca^{2+}]_i$) induced by ATP in BV-2 cells. Application of 100 μM ATP for 30 s induced a calcium response that was evaluated as the difference between the fluorescence ratio at the peak of the response and the basal ratio (Δ ratio) (Fig. 2*A*). In 77 cells recorded in 3 independent experiments, the increase of $[Ca^{2+}]_i$ corresponded to a mean Δ ratio of 0.24 ± 0.02 (Fig. 2*A*,*D*). Applications of 1 μM ionomycin evoked typical and reproducible rises of $[Ca^{2+}]_i$. Given that ivermectin selectively enhanced ATP-evoked $P2X_4$-current densities, we then examined the sensitivity of ATP-induced Ca^{2+} ion entry to ivermectin. Two minutes pretreatment with 3 μM ivermectin strongly potentiated the calcium response to 100 μM ATP (Δ ratio = 0.55 ± 0.05, $n = 71$) (Fig. 2*B*,*D*). The rise of fluorescence ratio induced by ATP was increased by 229%. Depletion of PIP_2 and PIP_3 levels by preincubation with 35 μM wortmannin (PI3K and PI4K blockade) for 10 min significantly decreased the $P2X_4$-mediated calcium entry (Δ ratio: 0.32 ± 0.04, $n = 45$) (Fig. 2*C*,*D*). The responses to ionomycin were similar in BV-2 cells exposed to wortmannin plus ivermectin compared with those exposed to ivermectin alone (Δ ratio = 0.24 ± 0.02, $n = 45$ and 0.28 ± 0.02, $n = 71$, respectively). Using published calibration methods (Grynkiewicz et al., 1985), we estimated the rise of $P2X_4$-mediated $[Ca^{2+}]_i$ at 240 ± 10 nM for vehicle-treated cells, 650 ± 70 nM for cells treated with 3 μM ivermectin, and 360 ± 30 nM for cells treated with both 3 μM ivermectin and 35 μm wortmannin. Altogether, these results show that disrupting PIP_2 and PIP_3 levels significantly decrease the capacity of $P2X_4$ channels to mediate calcium entry into microglial cells.

$P2X_4$ current amplitude is decreased by wortmannin treatment in *Xenopus* oocytes

To further investigate the modulation of $P2X_4$ currents by phosphoinositides, we conducted experiments on *Xenopus* oocytes expressing recombinant $P2X_4$ receptor channels. Oocytes were incubated for 2 h in wortmannin at 100 nM (PI3K blockade), or at 35 μM (PI3K and PI4K blockade). The amplitude of the first evoked $P2X_4$ current was recorded (Fig. 3). The average current amplitude in control conditions was 4.2 ± 0.6 μA ($n = 6$). As shown in Figure 3, *A* and *B*, 100 nM wortmannin induced a significant decrease of ~50% in the $P2X_4$ current amplitude, down to 2.1 ± 0.6 μA ($p = 0.0347$, $n = 6$), whereas 35 μM wortmannin led to an even greater inhibition of $P2X_4$ current amplitude (0.8 ± 0.4 μA; $p = 0.0007$, $n = 7$). Dose–response curves confirmed a fourfold decrease in maximal current amplitudes after treatment with wortmannin (Fig. 3*C*). They also revealed a small albeit significant increase in the EC_{50} of ATP (18.7 ± 1.8 μM in vehicle-treated oocytes, 28.7 ± 2.4 μM in wortmannin-treated oocytes, $n = 4$–9, $^*p < 0.05$).

Impact of phosphoinositides on the speed of recovery of $P2X_4$ currents

We then tested whether the depletion of PIP_2 or PIP_3 could affect the speed of recovery of $P2X_4$-mediated currents. We activated the receptor with three successive applications of 100 μM ATP at 4 min intervals, and measured the amplitude of the third current relative to the first current response, defined as the third/first recovery ratio. Under control conditions, a 4 min washout between each agonist application was enough for the receptor to fully recover: the third/first ratio was of 100 ± 8% ($n = 7$) (Fig. 4*A*). Blocking PIP_3 synthesis with 100 nM wortmannin preincubation led to a gradual decrease of the currents, the amplitude of the third currents being 66 ± 11% of that of the initial current

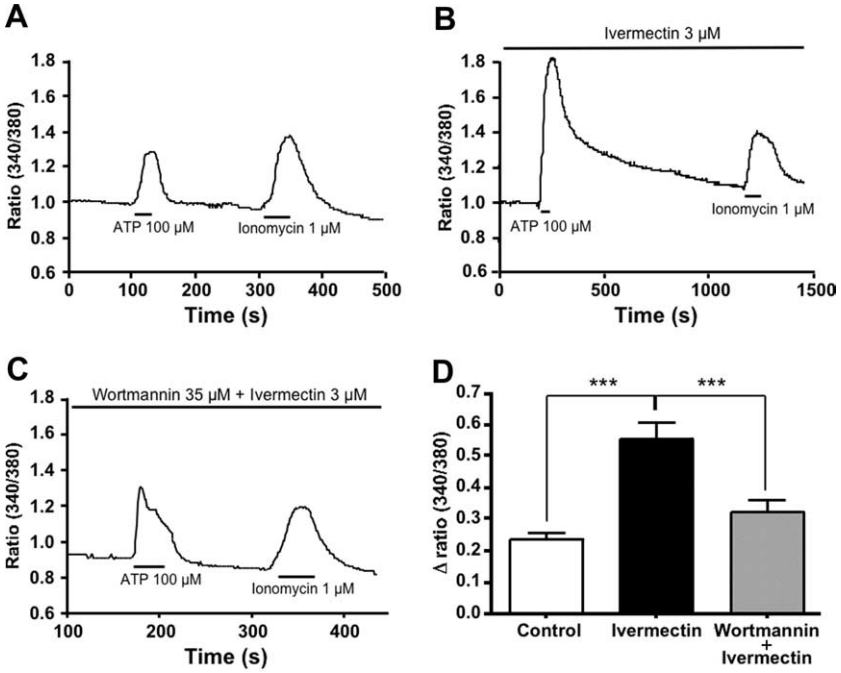

Figure 2. Wortmannin treatment leads to a decrease in ATP-induced calcium entry in BV-2 cells. ***A–C***, Representative recordings of calcium-mediated fura-2 fluorescence (340/380 nm ratio) over time in BV-2 cells in response to 100 μM ATP. ***A***, In control conditions, a BV-2 cell was challenged with 100 μM ATP during 30 s. ***B***, Before ATP application, 2 min preapplication of 3 μM ivermectin strongly increased the ATP-induced $[Ca^{2+}]_i$ increase. ***C***, Ten minutes of preincubation of BV-2 cell with 35 μM wortmannin led to a decrease in ATP-induced calcium entry. Cells were challenged with 1 μM ionomycin to test their viability at the end of recordings. ATP, ivermectin, and ionomycin were applied by superfusion at the times indicated by the horizontal bars. ***D***, Quantitation of the amplitude of responses to 100 μM ATP, measured by the Δ ratio (see Materials and Methods). Error bars represent mean ± SEM of 3 independent experiments. White bar: mean amplitude of ATP response under control conditions ($n = 77$). Black bar: mean amplitude of ATP response after perfusion with 3 μM ivermectin ($n = 71$). Gray bar: mean amplitude of ATP response after preincubation with 35 μM wortmannin (gray bar, $n = 45$) and perfusion with 3 μM ivermectin. Significance was determined by ANOVA using Bonferroni's multiple comparison test. ***$p < 0.001$.

(Fig. 4*B*). When both PIP_2 and PIP_3 levels were depleted with 35 μM wortmannin preincubation, the third current went down to 26 ± 5% of the first one (Fig. 4*C*). The third/first ratios under both 100 nM and 35 μM wortmannin were significantly smaller than under control conditions ($p = 0.0251$, $n = 6$ and $p < 0.0001$, $n = 7$, respectively).

Injection of phosphoinositides rescues $P2X_4$ current amplitude in wortmannin-treated oocytes

To test the selective involvement of phosphoinositides in the modulation of $P2X_4$ channel responses by wortmannin, we conducted experiments in which diC_8-PIP_2 or diC_8-PIP_3 were injected into the oocyte cytoplasm. Initial channel activation was recorded, followed by injection of vehicle (PBS) or phosphoinositides, to reach an intracellular concentration of 200 μM. The subsequent current activation was then recorded and compared with preinjection amplitude. Notably, under basal conditions, injection of either diC_8-PIP_2 or diC_8-PIP_3 did not lead to any change in the $P2X_4$ current amplitude (data not shown), suggesting that PIP_2 and PIP_3 levels are saturating under basal conditions. However, injection of phosphoinositides rescued $P2X_4$ current amplitudes in conditions of wortmannin-induced depletion (Fig. 5*A*,*B*). As shown in Figure 5*C*, diC_8-PIP_3 injection induced a 396 ± 64% increase in $P2X_4$ ($p = 0.012$, $n = 4$), whereas diC_8-PIP_2 injection led to a 827 ± 244% increase ($p = 0.006$, $n = 4$).

$P2X_4$ current kinetics is sensitive to PIP_2 levels

To assess changes in $P2X_4$ current kinetics in *Xenopus* oocytes, we examined the activation rate, calculated as the 10–90% rise time of the onset current, and the desensitization rate calculated as the monoexponential fit of the inactivation current phase (Fig. 6*A*). Preincubation with 35 μM wortmannin (PI3K and PI4K blockade) induced an increase of the 10–90% rise time (1.15 ± 0.1 s, $p = 0.0068$, $n = 7$) compared with vehicle-treated oocytes (0.72 ± 0.08 s, $n = 10$) indicative of a slower activation rate of $P2X_4$ channels (Fig. 6*B*,*C*). The 10–90% rise time was not affected by treatment with 100 nM wortmannin (PI3K blockade) (0.59 ± 0.06 s, $n = 7$). The same kinetics parameter was studied at 35 μM wortmannin followed by injection of diC_8-PIP_2 or vehicle. Under these conditions, cytoplasmic diC_8-PIP_2 injection led to a faster activation rate compared with vehicle-injected oocytes, with respective rise times of 0.90 ± 0.07 s and 1.61 ± 0.28 s respectively ($p = 0.0263$, $n = 13$–14).

The desensitization rate of $P2X_4$-mediated currents was studied under similar experimental conditions. Vehicle-treated oocytes showed a desensitization rate of 6.73 ± 0.85 s, whereas preincubation with 35 μM wortmannin slowed it significantly to 15.76 ± 2.8 s ($p = 0.0089$, $n = 5$–6). Under these conditions, cytoplasmic diC_8-PIP_2 injection led to a faster desensitization rate compared with that of vehicle-injected oocytes, with inactivation times of 5.15 ± 0.34 s and 9.17 ± 0.59 s respectively ($p < 0.0001$, $n = 13$–17). A treatment with 100 nM wortmannin did not modify the desensitization rate of $P2X_4$ currents (6.23 ± 1.96 s, $n = 6$).

PIP_2 activates $P2X_4$ current responses in excised inside-out macropatches

Excised inside-out patch recordings were performed to test the direct effects of phosphoinositides on heterologously expressed $P2X_4$ channels. Upon patch excision, a fast rundown of the current was observed. Application of 100 μM polylysine, which sequesters endogenous anionic phospholipids, induced a further rundown of the residual current. Subsequent application of 5 μM diC_8-PIP_2 to the intracellular side of the membrane activated $P2X_4$ currents (Fig. 7*A*,*B*). A quantitative analysis shows a significantly larger $P2X_4$ current amplitude (~1.7-fold increase, $p = 0.0059$) in the presence of diC_8-PIP_2 (32 ± 6 pA, $n = 7$) compared with rundown baseline levels (19 ± 4 pA, $n = 7$).

A proximal C-terminal sequence of $P2X_4$ subunit is critical for phosphoinositide binding

Phosphoinositides are negatively charged lipids so we investigated potential interactions with basic residues on the intracellular domain of the $P2X_4$ channel subunit, using a lipid strip assay. The proximal region of the C-terminal domain displays a cluster of basic amino acids potentially involved in the interaction with

phosphoinositides. A $P2X_4$ peptide containing the sequence C_{360}–V_{375} (Fig. 8*A*) was expressed as a GST-fusion protein, whereas GST protein alone was used as negative control for the lipid binding assay. No specific binding was observed when the GST protein alone or GST fused with the N-terminal sequence F_{12}–V_{29} was tested (Fig. 8*B*). However the GST–$P2X_4$ (C_{360}–V_{375}) construct selectively bound to several phosphatidylinositides including PI(3)P, PI(4)P, PI(5)P, $PI(3,4)P_2$, $PI(3,5)P_2$, PIP_2, and PIP_3. It also showed strong binding to phosphatidylserine and phosphatidic acid. The neutral lipids phosphatidylethanolamine and phosphatidylcholine did not display any affinity for the GST–$P2X_4$ (C_{360}–V_{375}) construct.

Discussion

We demonstrate here a specific modulation of $P2X_4$ receptor function by phosphoinositides. This modulation is physiologically relevant as both native $P2X_4$ currents and $P2X_4$-mediated calcium entry are sensitive to PIP_2 and PIP_3 levels in microglial cells. Microglia are immunocompetent cells that respond to adverse conditions in the CNS, such as neurodegeneration, trauma, ischemia, inflammation, and infection. Increasing evidence indicate that microglia also play a critical role in the pathogenesis of neuropathic pain, a debilitating chronic condition that can occur after peripheral nerve damage. After nerve injury, microglia located in the ipsilateral dorsal horn of spinal cord become activated and upregulate the expression of $P2X_4$ subunit (Tsuda et al., 2003). Recent findings suggest that ATP-induced activation of microglia evokes the release of BDNF and downregulation of the neuronal cotransporter KCC2, leading to postsynaptic changes in the electrochemical gradient of chloride ions and disinhibition (Coull et al., 2003, 2005). BV-2 cells have been established as a model of murine microglia. Native microglial cultures have serious limitations including short survival time *ex vivo*, heterogeneity in activation states (Lawson et al., 1990; Ren et al., 1999) and the process of isolating primary microglia can result in phenotypical changes (Frank et al., 2006). $P2X_4$ and $P2X_7$ are the major P2X subtypes expressed in BV-2 cells (Raouf et al., 2007). We successfully isolated $P2X_4$ currents from $P2X_7$ currents by using a dual pharmacological strategy based on the higher sensitivity of mouse $P2X_4$ to ATP compared with that of mouse $P2X_7$ (Townsend-Nicholson et al., 1999; Raouf et al., 2007) and on the use of ivermectin, a selective allosteric potentiator of $P2X_4$-containing receptors (Khakh et al., 1999; Toulmé et al., 2006). Our patch-clamp recordings data showed reduced $P2X_4$ current density after blockade of PI3K and PI4K with wortmannin at 100 nM and 35 μM, respectively. The ATP-induced microglial release of the proalgesic cytokines TNF-α and interleukin-6 involve Ca^{2+}-dependent pathways (Hide et al., 2000; Shigemoto-Mogami et al., 2001; Hanisch, 2002). $P2X_4$ receptor channels are

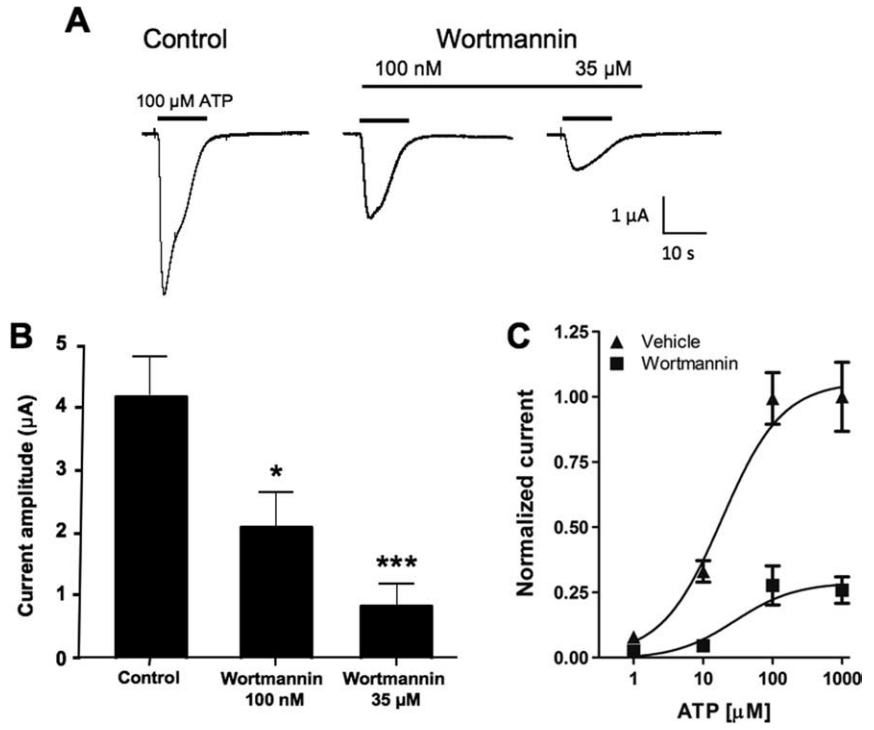

Figure 3. Blocking phosphoinositides synthesis leads to a decrease in $P2X_4$ current amplitude in *Xenopus* oocytes. ***A***, Sample traces showing ATP-gated currents in oocytes expressing $P2X_4$ after vehicle or 100 nM or 35 μM wortmannin treatment. ***B***, Quantitative results. $P2X_4$ currents have an average amplitude of $4.17 \pm 0.64\mu$A ($n = 6$) in oocytes incubated in control solution (Barth's solution with DMSO) while blocking PI3K with 100 nM wortmannin decreased $P2X_4$ current amplitude to $2.09 \pm 0.57\ \mu$A ($p = 0.0347$, $n = 6$). Blocking both PI3K and PI4K with 35 μM wortmannin decreased current amplitudes to $0.83 \pm 0.38\ \mu$A ($p = 0.0007$, $n = 7$). ***C***, Normalized ATP concentration-current amplitude curves in absence (vehicle) or in presence of 35 μM wortmannin. Wortmannin decreases the maximal current amplitude and increases the EC_{50} of ATP ($n = 4$–9).

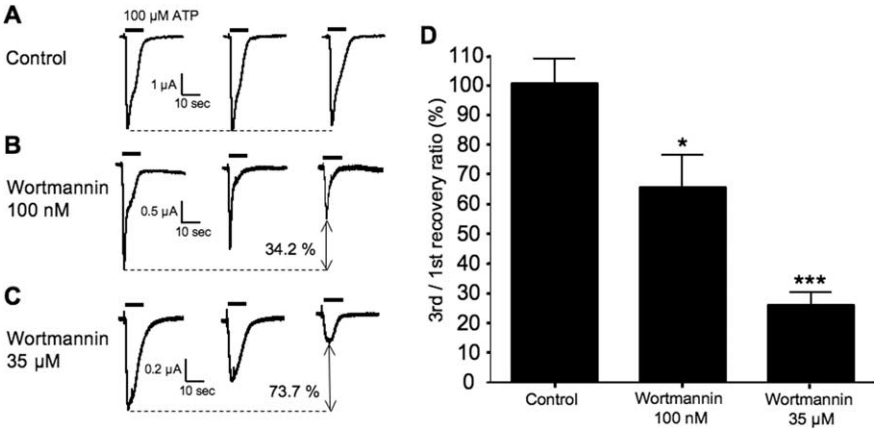

Figure 4. Phosphoinositides depletion leads to decreased recovery of $P2X_4$ currents during successive activations with ATP. In *Xenopus* oocytes expressing $P2X_4$, we measured the currents induced by three successive applications of 100 μM ATP, at 4 min intervals. Rundown of currents is measured as the ratio of the amplitude of the third response over that of the first. Shown here are sample traces of a recording series after incubation in vehicle (***A***), 100 nM wortmannin (***B***), and 35 μM wortmannin (***C***). ***D***, Under control conditions, the third current amplitude was $100.4 \pm 8.3\%$ ($n = 7$) of the first, i.e., complete recovery of the receptor was observed. After 2 h incubation in 100 nM wortmannin, currents recovered to $65.8 \pm 10.8\%$ ($p = 0.025$, $n = 6$) and to $26.3 \pm 4.7\%$ ($p < 0.001$, $n = 7$) after 35 μM wortmannin incubation.

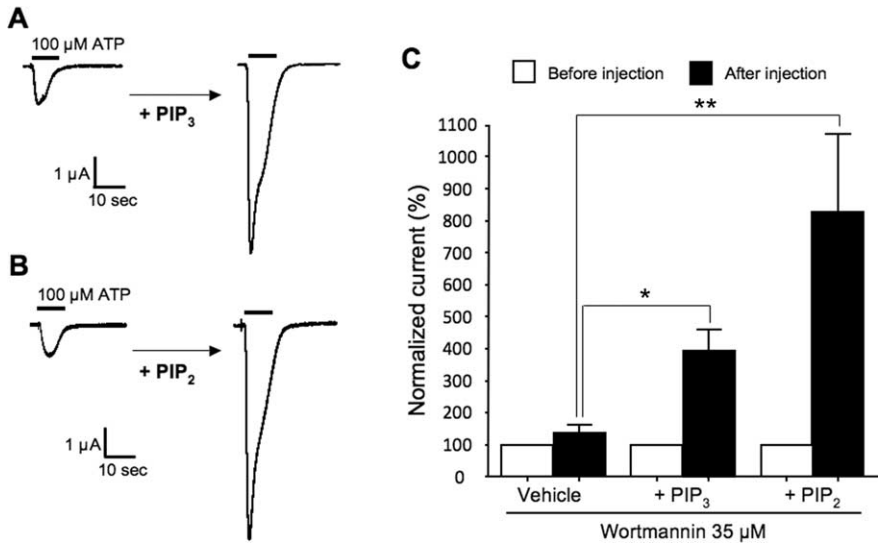

Figure 5. Injection of PIP_2 and PIP_3 rescues $P2X_4$ current amplitude under conditions of wortmannin-induced phosphoinositide depletion. Oocytes expressing $P2X_4$ were incubated in 35 μM wortmannin, and ATP-evoked currents were then recorded before and after phosphoinositide injection. Sample traces showing the effect of the injection of diC_8-PIP_3 (***A***) or diC_8-PIP_2 (***B***) compared with the preinjection current. ***C***, Quantitative data show that, after phosphoinositide depletion with wortmannin, injection of diC_8-PIP_3 leads to a 396 ± 64% ($p = 0.012$, $n = 4$) increase of the $P2X_4$ response to 100 μM ATP, and injection of diC_8-PIP_2 increases the currents by 827 ± 244% ($p = 0.006$, $n = 4$). Injection of vehicle (PBS) did not induce any significant change on the $P2X_4$ currents ($n = 7$).

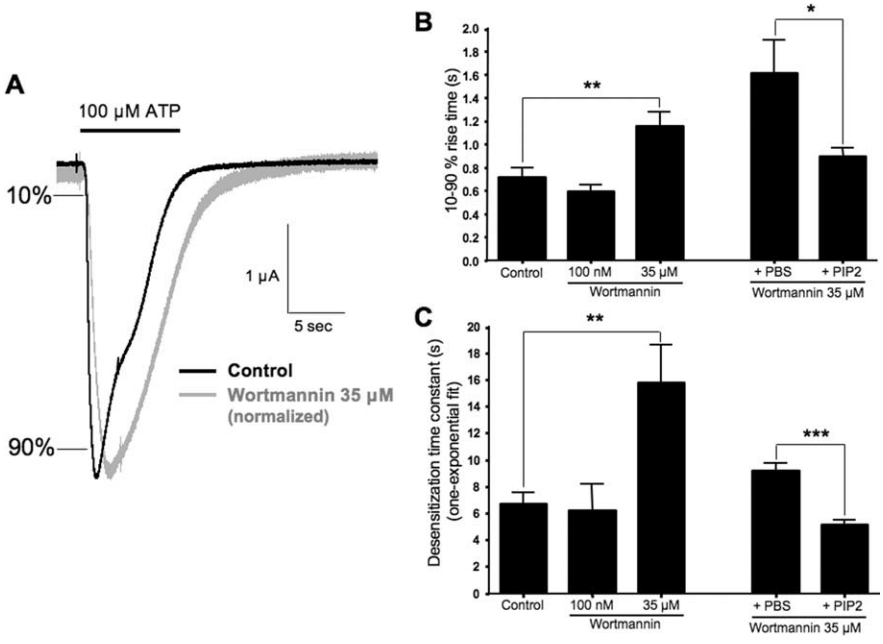

Figure 6. Phosphoinositide depletion leads to changes in the kinetics of $P2X_4$ currents in *Xenopus* oocytes. ***A***, Sample traces showing the typical kinetics of $P2X_4$ currents, under control conditions and after a 2 h treatment with 35 μM wortmannin. ***B***, Quantitative results for $P2X_4$ current 10–90% rise times. Incubation of the oocytes in 35 μM wortmannin, but not in 100 nM wortmannin, led to an increase in the rise time ($p = 0.0069$, $n = 7$–10) and injection of diC_8-PIP_2 normalized the rise time ($p = 0.026$, $n = 13$–14). ***C***, Quantitative results for the desensitization time constants. Incubation in 35 μM wortmannin, but not in 100 nM wortmannin, led to an increase in the desensitization time ($p = 0.0089$, $n = 5$–6). After incubation in 35 μM wortmannin, injection of diC_8-PIP_2 decreased the desensitization time significantly compared with the injection of vehicle (PBS) ($p < 0.0001$, $n = 13$–17).

highly permeable to Ca^{2+} ions (Egan and Khakh, 2004) and we used this property to measure in ratiometric imaging a significant reduction of ATP-induced ivermectin-sensitive Ca^{2+} ion entry after treatment with wortmannin. Altogether, our results show that both PIP_2 and PIP_3 levels regulate the activity of native $P2X_4$ receptor channels in BV-2 microglial cells. It is possible that a large Ca^{2+} influx through $P2X_4$ receptor channels could activate Ca^{2+}-dependent isoforms of phospholipase C, leading to decreased PIP_2 levels and subsequent decreased channel responses. Interestingly, such a mechanism of Ca^{2+}-induced inactivation of PIP_2-sensitive channels through activation of phospholipase C has been described recently for TRP channels (Rohács et al., 2005; Thyagarajan et al., 2008).

The modulation of $P2X_4$ responses by phosphoinositides does not depend on a cell-specific context since we reconstituted it in the *Xenopus* oocyte expression system. Wortmannin-induced phosphoinositides depletion in oocytes led to reduced maximal $P2X_4$ currents, lower sensitivity to ATP, longer recovery times following repeated agonist applications, as well as slower current activation and inactivation kinetics. We conclude that ATP becomes a partial agonist for $P2X_4$ when PIP_2 and PIP_3 levels are depleted, i.e., phosphoinositides are required cofactors for the full expression of $P2X_4$ function. Treatment with wortmannin at micromolar concentrations could potentially affect many intracellular pathways. However we validated the selective blockade of phosphoinositides synthesis by normalizing $P2X_4$ current amplitude as well as kinetics with cytoplasmic injections of PIP_2 or PIP_3. Interestingly, depleting PIP_3 levels has an impact on the amplitude of $P2X_4$ currents and on their recovery time, but not on their kinetics of activation or inactivation which are sensitive to PIP_2 only. Therefore $P2X_4$ channels are sensitive to both PIP_2 and PIP_3 albeit through different mechanisms of regulation.

Although earlier studies conducted on the modulation of ion channels by phosphoinositides showed a predominant role of PIP_2 as a signaling molecule (Suh and Hille, 2008), there is increasing evidence that PIP_3 also regulates various ion channels including K^+ inward rectifier channels (Rohács et al., 2003), Ca^{2+}-activated K^+ channels (Srivastava et al., 2005), epithelial Na^+ channels (Pochynyuk et al., 2006) as well as cyclic nucleotide-gated channels (Zhainazarov et al., 2004). Among the P2X receptors, the desensitization of the $P2X_2$ subtype is modulated by PI(3)P and PI(3,5)P_2 (Fujiwara and Kubo, 2006) and we have recently reported that the $P2X_1$ and $P2X_7$ subtypes are sensitive to PIP_2, but not to PIP_3 (Zhao et al., 2007; Bernier et al., 2008). Therefore the sensitivity of $P2X_4$ receptor channels to both PIP_2 and PIP_3 indicates that phosphoinositides regulate P2X receptor channel function in a subunit-specific manner.

We also provide evidence that modulation of $P2X_4$ channels

results from the direct effects of protein-lipid interactions on channel function, and not from indirect effects on trafficking and endocytosis since PIP_2 is able to rescue $P2X_4$ currents from rundown in inside-out macropatches excised from oocytes. $P2X_4$ channel activity was stimulated by direct application of PIP_2 to the intracellular side of the macropatch, likely by promoting the exit of $P2X_4$ channels from their desensitized state. This could explain the longer recovery time and the slower kinetics of $P2X_4$ currents recorded in whole cell configuration when PIP_2 levels are low after treatment with wortmannin. Another strong argument for the direct effect of phospholipids on $P2X_4$ function is based on the fact that PIP_2 and PIP_3, as well as other phosphoinositides, are able to interact directly with the proximal C-terminal subdomain Cys_{360}–Val_{375} of $P2X_4$ subunits *in vitro*. This region contains a cluster of basic residues at the right location for interacting with membrane-bound anionic phospholipids, and it shows significant conservation among all known P2X subunits. By analogy with other channels (Suh and Hille, 2008), the highly negatively charged head group in phosphoinositides is thought to interact directly with a distinct positively charged binding site in this region of the $P2X_4$ subunit. The exact contribution of each of the 7 candidate residues (6 lysines and 1 arginine, see sequence in Fig. 8) to the binding of PIP_2 and/or PIP_3 will remain to be investigated.

The fact that the N-terminal domain of $P2X_4$ did not bind to any of the phosphoinositides tested confirms an important regulatory role for the C-terminal domain that also contains determinants of desensitization (Fountain and North, 2006) and internalization (Royle et al., 2005). Our results in macropatch recordings and in lipid binding assay strongly suggest that direct interactions between $P2X_4$ channels and phosphoinositides mediate the modulation observed in microglia as well as in *Xenopus* oocytes.

The relevance of the modulation of microglial and neuronal $P2X_4$ function by PIP_2 and/or PIP_3 in pathophysiological conditions like neuropathic pain will remain to be established. However, in a broader context, our results highlight a positive and subunit-specific modulation of P2X receptor channels by phosphoinositides through direct channel–lipid interactions. Many metabotropic receptors regulate phosphoinositide levels through the activation of PI3K or phospholipase C, therefore we will need to integrate their

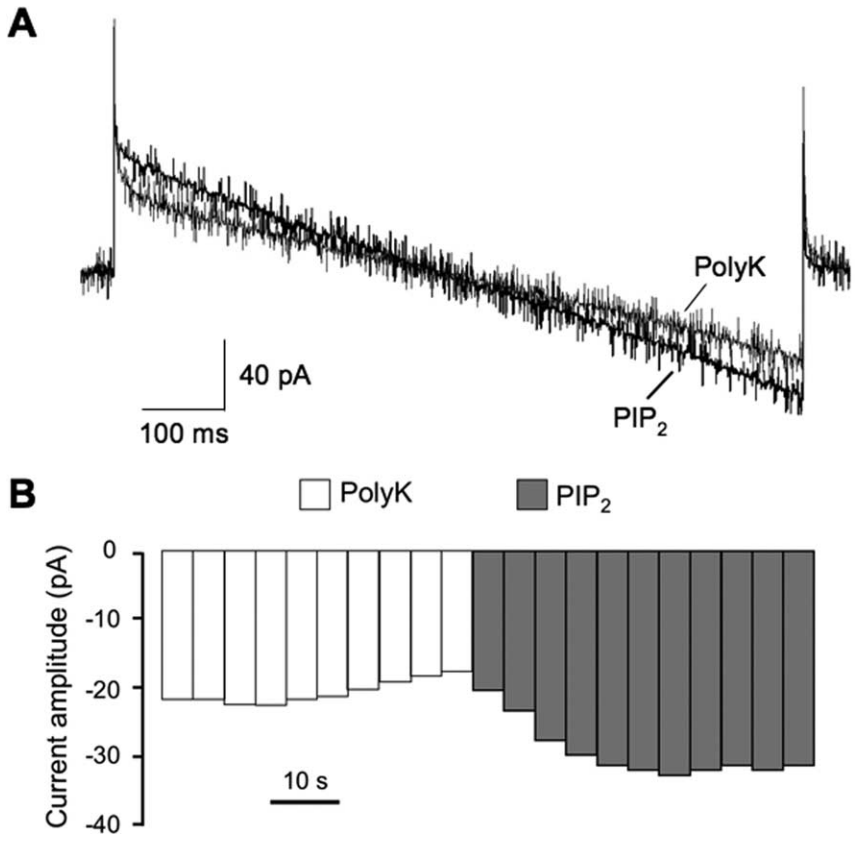

Figure 7. PIP_2 activates $P2X_4$ currents in inside-out macropatches excised from *Xenopus* oocytes. The macropatch pipette solution contained 100 μM ATP. ***A***, Typical $P2X_4$ currents recorded during 1 s voltage ramps from +100 mV to −100 mV. The chelator poly-Lysine (polyK) was applied at 100 μM and the phospholipid diC_8-PIP_2 (PIP_2) was applied at 5 μM. ***B***, Time course of averaged peak currents measured at −80 mV during 5 s intervals.

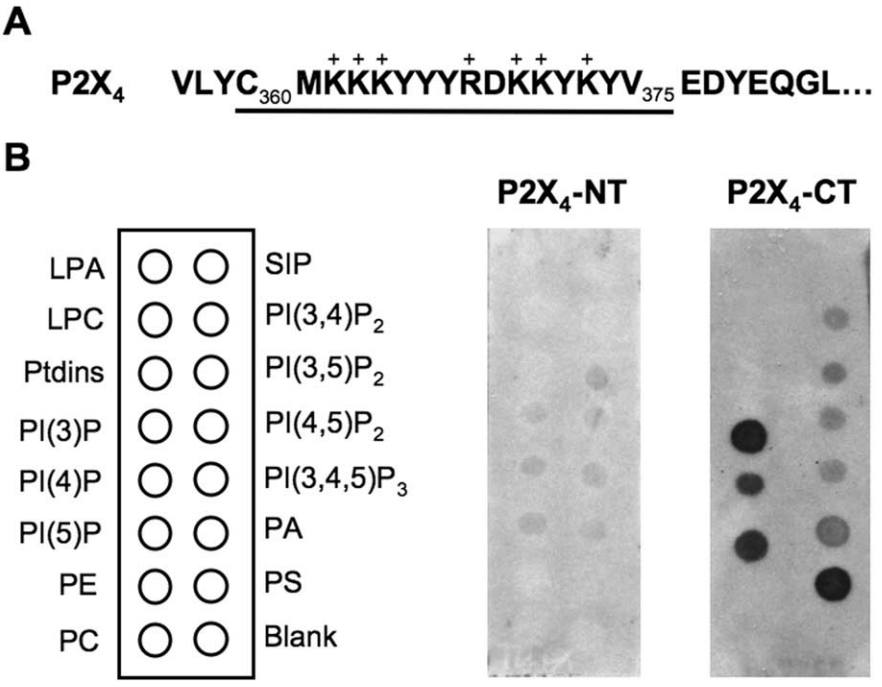

Figure 8. Direct binding of phosphoinositides to the $P2X_4$ C-terminal domain. ***A***, Primary structure of the proximal C terminus of rat $P2X_4$ subunit showing intracellular lysine and arginine residues candidate for phospholipid binding. ***B***, Specific phospholipid-binding pattern of the GST-tagged 16 aa C-terminal $P2X_4$ peptide C_{360}–V_{375}. The C-terminal peptide binds directly to several biologically active phosphoinositides including PI(3)P, PI(4)P, PI(5)P, $PI(3,4)P_2$, $PI(3,5)P_2$, PIP_2, and PIP_3 ($n = 6$).

exact role on P2X function in our understanding of ionotropic ATP signaling in the nervous system and in peripheral tissues.

References

Bernier LP, Ase AR, Tong X, Hamel E, Blais D, Zhao Q, Logothetis DE, Séguéla P (2008) Direct modulation of P2X1 receptor-channels by the lipid phosphatidylinositol 4,5-bisphosphate. Mol Pharmacol 74:785–792.

Coull JA, Boudreau D, Bachand K, Prescott SA, Nault F, Sík A, De Koninck P, De Koninck Y (2003) Trans-synaptic shift in anion gradient in spinal lamina I neurons as a mechanism of neuropathic pain. Nature 424:938–942.

Coull JA, Beggs S, Boudreau D, Boivin D, Tsuda M, Inoue K, Gravel C, Salter MW, De Koninck Y (2005) BDNF from microglia causes the shift in neuronal anion gradient underlying neuropathic pain. Nature 438:1017–1021.

Egan TM, Khakh BS (2004) Contribution of calcium ions to P2X channel responses. J Neurosci 24:3413–3420.

Fountain SJ, North RA (2006) A C-terminal lysine that controls human P2X4 receptor desensitization. J Biol Chem 281:15044–15049.

Frank MG, Wieseler-Frank JL, Watkins LR, Maier SF (2006) Rapid isolation of highly enriched and quiescent microglia from adult rat hippocampus: immunophenotypic and functional characteristics. J Neurosci Methods 151:121–130.

Fujiwara Y, Kubo Y (2006) Regulation of the desensitization and ion selectivity of ATP-gated P2X2 channels by phosphoinositides. J Physiol 576:135–149.

Grynkiewicz G, Poenie M, Tsien RY (1985) A new generation of calcium indicators with greatly improved fluorescence properties. J Biol Chem 260:3440–3450.

Guo C, Masin M, Qureshi OS, Murrell-Lagnado RD (2007) Evidence for functional P2X4/P2X7 heteromeric receptors. Mol Pharmacol 72:1447–1456.

Hanisch UK (2002) Microglia as a source and target of cytokines. Glia 40:140–155.

Hide I, Tanaka M, Inoue A, Nakajima K, Kohsaka S, Inoue K, Nakata Y (2000) Extracellular ATP triggers tumor necrosis factor-alpha release from rat microglia. J Neurochem 75:965–972.

Hilgemann DW, Feng S, Nasuhoglu C (2001) The complex and intriguing lives of PIP2 with ion channels and transporters. Sci STKE 2001:RE19.

Inoue K, Tsuda M, Koizumi S (2004) ATP- and adenosine-mediated signaling in the central nervous system: chronic pain and microglia: involvement of the ATP receptor P2X4. J Pharmacol Sci 94:112–114.

Khakh BS, Proctor WR, Dunwiddie TV, Labarca C, Lester HA (1999) Allosteric control of gating and kinetics at $P2X_4$ receptor channels. J Neurosci 19:7289–7299.

Lawson LJ, Perry VH, Dri P, Gordon S (1990) Heterogeneity in the distribution and morphology of microglia in the normal adult mouse brain. Neuroscience 39:151–170.

Lê KT, Babinski K, Séguéla P (1998) Central P2X4 and P2X6 channel subunits coassemble into a novel heteromeric ATP receptor. J Neurosci 18:7152–7159.

Nakanishi S, Catt KJ, Balla T (1995) A wortmannin-sensitive phosphatidylinositol 4-kinase that regulates hormone-sensitive pools of inositolphospholipids. Proc Natl Acad Sci U S A 92:5317–5321.

Nicke A, Kerschensteiner D, Soto F (2005) Biochemical and functional evidence for heteromeric assembly of P2X1 and P2X4 subunits. J Neurochem 92:925–933.

North RA (2002) Molecular physiology of P2X receptors. Physiol Rev 82:1013–1067.

Pochynyuk O, Tong Q, Staruschenko A, Ma HP, Stockand JD (2006) Regulation of the epithelial Na+ channel (ENaC) by phosphatidylinositides. Am J Physiol Renal Physiol 290:F949–F957.

Priel A, Silberberg SD (2004) Mechanism of ivermectin facilitation of human P2X4 receptor channels. J Gen Physiol 123:281–293.

Raouf R, Chabot-Doré AJ, Ase AR, Blais D, Séguéla P (2007) Differential regulation of microglial P2X4 and P2X7 ATP receptors following LPS-induced activation. Neuropharmacology 53:496–504.

Ren L, Lubrich B, Biber K, Gebicke-Haerter PJ (1999) Differential expression of inflammatory mediators in rat microglia cultured from different brain regions. Mol Brain Res 65:198–205.

Rohács T, Lopes CM, Jin T, Ramdya PP, Molnár Z, Logothetis DE (2003) Specificity of activation by phosphoinositides determines lipid regulation of Kir channels. Proc Natl Acad Sci U S A 100:745–750.

Rohács T, Lopes CM, Michailidis I, Logothetis DE (2005) $PI(4,5)P_2$ regulates the activation and desensitization of TRPM8 channels through the TRP domain. Nat Neurosci 8:626–634.

Rosenhouse-Dantsker A, Logothetis DE (2007) Molecular characteristics of phosphoinositide binding. Pflugers Arch 455:45–53.

Royle SJ, Qureshi OS, Bobanović LK, Evans PR, Owen DJ, Murrell-Lagnado RD (2005) Non-canonical YXXGPhi endocytic motifs: recognition by AP2 and preferential utilization in P2X4 receptors. J Cell Sci 118:3073–3080.

Rubio ME, Soto F (2001) Distinct localization of P2X receptors at excitatory postsynaptic specializations. J Neurosci 21:641–653.

Shigemoto-Mogami Y, Koizumi S, Tsuda M, Ohsawa K, Kohsaka S, Inoue K (2001) Mechanisms underlying extracellular ATP-evoked interleukin-6 release in mouse microglial cell line, MG-5. J Neurochem 78:1339–1349.

Srivastava S, Li Z, Lin L, Liu G, Ko K, Coetzee WA, Skolnik EY (2005) The phosphatidylinositol 3-phosphate phosphatase myotubularin-related protein 6 (MTMR6) is a negative regulator of the Ca2+-activated K+ channel KCa3.1. Mol Cell Biol 25:3630–3638.

Suh BC, Hille B (2005) Regulation of ion channels by phosphatidylinositol 4,5-bisphosphate. Curr Opin Neurobiol 15:370–378.

Suh BC, Hille B (2008) PIP2 is a necessary cofactor for ion channel function: how and why? Annu Rev Biophys 37:175–195.

Thyagarajan B, Lukacs V, Rohacs T (2008) Hydrolysis of phosphatidylinositol 4,5-bisphosphate mediates calcium-induced inactivation of TRPV6 channels. J Biol Chem 283:14980–14987.

Toulmé E, Soto F, Garret M, Boué-Grabot E (2006) Functional properties of internalization-deficient P2X4 receptors reveal a novel mechanism of ligand-gated channel facilitation by ivermectin. Mol Pharmacol 69:576–587.

Townsend-Nicholson A, King BF, Wildman SS, Burnstock G (1999) Molecular cloning, functional characterization and possible cooperativity between the murine P2X4 and P2X4a receptors. Brain Res Mol Brain Res 64:246–254.

Trang T, Beggs S, Salter MW (2006) Purinoceptors in microglia and neuropathic pain. Pflugers Arch 452:645–652.

Tsuda M, Shigemoto-Mogami Y, Koizumi S, Mizokoshi A, Kohsaka S, Salter MW, Inoue K (2003) P2X4 receptors induced in spinal microglia gate tactile allodynia after nerve injury. Nature 424:778–783.

Vanhaesebroeck B, Leevers SJ, Ahmadi K, Timms J, Katso R, Driscoll PC, Woscholski R, Parker PJ, Waterfield MD (2001) Synthesis and function of 3-phosphorylated inositol lipids. Annu Rev Biochem 70:535–602.

Zhainazarov AB, Spehr M, Wetzel CH, Hatt H, Ache BW (2004) Modulation of the olfactory CNG channel by Ptdlns(3,4,5)P3. J Membr Biol 201:51–57.

Zhao Q, Yang M, Ting AT, Logothetis DE (2007) PIP_2 regulates the ionic current of P2X receptors and $P2X_7$ receptor-mediated cell death. Channels 1:46–55.